PROCEEDINGS of the
23rd International Congress on Acoustics

9 to 13 September 2019 in Aachen, Germany

Anisotropic sound fields in reverberation-room measurements of sound absorption coefficients: Wavenumber spectrum theory

Mélanie NOLAN[1]

Acoustic Technology, Department of Electrical Engineering, Technical University of Denmark,

Ørsteds Plads, Building 352, 2800 Kgs. Lyngby, Denmark and Saint-Gobain Ecophon, 265 75 Hyllinge, Sweden

ABSTRACT

Measured values of absorption coefficients obtained from standardized reverberation-chamber measurements often differ across laboratories, mainly due to non-isotropic sound incidence on the absorbing specimen, and differences in the chambers' shapes and dimensions. The present study describes an experimental method for characterizing sound field isotropy in reverberation rooms. The methodology relies on a plane wave decomposition (i.e., estimation of the wavenumber spectrum) to describe the directional properties of the sound field in the vicinity of the absorbing specimen. By separating the incident from the reflected components in the wavenumber spectrum, it is possible to characterize the distribution of sound incidence on the sample, and to infer angle-dependent absorption properties. Measurements are conducted in a reverberation room with absorbing material on the floor using a programmable robotic arm to scan the sound field. The results confirm that the distribution of sound incidence on the sample is not isotropic in the steady state. The measured angle-dependent absorption coefficients show good agreement with theoretical predictions.

Keywords: Sound absorption, Isotropy, Array processing

1. INTRODUCTION

In reverberation-room measurements of sound absorption coefficients, a large sample of the material under test is placed in a reverberation room, and the absorption coefficient is deduced from the resulting reduction of the reverberation time, once the absorber has been introduced in the room [1]. The procedure is based on the simple reverberation formulas [2,3] for which a completely diffuse sound field must be established in the test chamber. An ideal diffuse field can be defined as the superposition of an infinite set of plane waves with random phases and equal magnitudes, which directions of propagation are uniformly distributed over all angles of incidence. In such a sound field, the energy density is uniformly distributed in space and the energy flow is isotropic; i.e., the sound field is homogeneous and isotropic. The absorption properties of the sample are represented by a (random-incidence) absorption coefficient, which corresponds to the average fraction of power absorbed by the sample when sound is arriving on it equally from all directions; i.e., under the assumption of isotropic sound incidence.

The shortcomings of the measurement procedure have become increasingly evident as shown in numerous investigations [4-7]: several systematic comparisons of the absorption coefficients determined in a number of standardized laboratories resulted in the conclusion that the absorption coefficient of a given area of the same material can take virtually any value. A vast amount of literature has grown around the subject and shows that the major cause of difficulties with the reverberation-chamber measurement of sound absorption can be attributed to a lack of diffuseness of the sound field, resulting in non-isotropic sound incidence on the absorbing specimen. Considerable experimental effort has been spent on the problem of evaluating diffusion in reverberant sound fields, and numerous methods have been proposed. An account of various descriptors is presented by Schultz [8], and more recently by Jeong et al. [9]. In particular, a variety of methods have been proposed, where diffusion is described on the basis of the angular distribution of sound energy [10-17].

Over the past few decades, technical developments in sensing methods have facilitated the three-dimensional analysis of sound fields. In particular, microphone arrays are especially well suited for

[1]melnola@elektro.dtu.dk

applications where the sound waves impinge on the array from multiple directions. The idea of using an array of microphones to measure the diffusion of reverberation chambers goes back to 1959, when Schroeder suggested creating a microphone array by repeated reflections of a planar array at the sidewalls of a reverberation chamber [18]. Rather than an array dependent on the room symmetry, Ebeling sampled the sound field in a reverberation chamber at every point of a three-dimensional cubical grid, with the goal of measuring cross-correlation functions in the spatial-frequency domain [13]. More recently, Gover et al. [14] investigated how spherical microphone arrays can be used to characterize directional properties of reverberant sound fields. They adapted the method described in Ref. 11 to spherical microphone arrays and measured the directional distribution of acoustic energy by steering directional beams in every direction. Extending this approach, Berzborn et al. [16] recently introduced the concept of Directional Energy Decay Curves (DEDC) derived from measurements of directional impulse responses using a spherical microphone array. In Ref. 15, Nolan et al. proposed an experimental method for evaluating isotropy in reverberant spaces in the steady-state, based on an analysis of the wavenumber spectrum in the spherical harmonics domain. The underlying hypothesis is that, in a perfectly isotropic sound field, the wavenumber spectrum is spherically symmetric. The method does not require a specific array configuration, as the analysis in the spherical harmonics domain is performed on the wavenumber spectrum, which is defined over a sphere, and not on the recorded sound pressure directly. Besides, such spectral representation of the wave field can be used to examine the distribution of the incident acoustic energy on the measuring sample and to reconstruct the incident power flows over a three-dimensional domain [17]. The aim of the present paper is to summarize the main findings from Refs. 15 and 17 and to discuss the limitations of some aspects of the work.

2. WAVENUMBER SPECTRUM THEORY

A detailed account of the theory is given in Refs. 15 and 17, and only the main results will be summarized here.

2.1 Wavenumber spectrum and sound field isotropy

The conception that a given pressure field can be expressed uniquely as a superposition of elementary waves is central to the methods outlined in this paper. Such plane wave decomposition consists in applying a three-dimensional Fourier transform to a measured pressure field to estimate the *wavenumber spectrum* [19], which is a representation of the sound field in the spatial-frequency domain, or k-space:

$$\mathrm{p}(\mathbf{r}_m) = \iiint_{-\infty}^{+\infty} P(\mathbf{k}) e^{-\mathrm{j}(k_x x_m + k_y y_m + k_z z_m)} d\mathbf{k} \approx \sum_{l=1}^{L} \widetilde{P}(\mathbf{k}_l) e^{-\mathrm{j}\mathbf{k}_l \cdot \mathbf{r}_m}, \tag{1}$$

where the quantity $\mathrm{P}(\mathbf{k}) = |P(\mathbf{k})| e^{\mathrm{j}\phi(\mathbf{k})}$ is the wavenumber (or angular) spectrum, with $|P(\mathbf{k})|$ and $\phi(\mathbf{k})$ its magnitude and phase, respectively. Each plane wave is traveling in a direction specified by the wavenumber vector $\mathbf{k}$, which satisfies the condition $k^2 \geq k_x^2 + k_y^2$ with $k_x^2 + k_y^2 + k_z^2 = k^2 = \|\mathbf{k}\|^2$ (indicating that they are propagating waves).

The pressure field sampled at a discrete number R of receiver positions (with an array of microphones) can be expressed in matrix form as

$$\mathbf{p} = \mathbf{H}\mathbf{x}, \tag{2}$$

where $\mathbf{p} \in \mathrm{C}^R$ is the measured sound pressure vector, $\mathbf{x} \in \mathrm{C}^L$ is a complex coefficient vector containing the wavenumber spectrum $\widetilde{P}(\mathbf{k}_l)$ in Eq. (1), and $\mathbf{H} \in \mathrm{C}^{R \times L}$ is the transfer matrix containing the plane wave functions. The problem is typically underdetermined ($L > R$) and the estimation of $\mathbf{x}$ obtained via a regularized matrix pseudo-inverse [20].

In order to evaluate isotropy, the magnitude of the wavenumber spectrum at frequency $f = kc/(2\pi)$ is expanded into a series of spherical harmonics

$$\left|\widetilde{P}(\theta, \phi)\right| = \sum_{n=0}^{\infty} \sum_{m=-n}^{n} A_{mn}(k) Y_n^m(\theta, \phi), \tag{3}$$

where the complex coefficients $A_{mn}(k)$ can be calculated from the orthonormality relation of the spherical harmonics functions. The relative monopole strength ι =

$|A_{00}(k)|/\sum_{n=0}^{\infty}\sum_{m=-n}^{n}|A_{mn}(k)|$ determines the degree of isotropy [15].

2.2 Sound field separation and reconstruction

From the estimated solution $\hat{\mathbf{x}}$, it is possible to reconstruct the sound field anywhere in the domain (pressure, velocity, and sound intensity) [17]

$$\mathbf{p}_r = \mathbf{H}_r\hat{\mathbf{x}}, \tag{4}$$

where $\mathbf{p}_r \in C^K$ is the reconstructed sound pressure vector estimated at a set of K positions $\mathbf{r}_r$, and $\mathbf{H}_r \in C^{KxL}$ is the reconstruction matrix containing the plane wave functions evaluated at the reconstruction points $\mathbf{r}_r$. The particle velocity vector $\mathbf{u}_r$ can be calculated from Euler's equation of motion, and the active intensity vector is $\mathbf{I}_r = \frac{1}{2}Re\{p_r\mathbf{u}_r^*\}$, where the superscript * denotes the complex conjugate. Considering that $\hat{\mathbf{x}} = [\hat{\mathbf{x}}^{(i)}; \hat{\mathbf{x}}^{(r)}]$, the reconstruction can alternatively be based on the complex coefficient vector $\hat{\mathbf{x}}^{(i)} \in C^N$ and the propagation matrix $\mathbf{H}_r^{(i)} \in C^{KxN}$ containing the wave components that describe the incident sound field (where N is the number of waves conforming the incident sound field). In this case, the reconstruction provides a complete characterization of the incident acoustic field (sound pressure $p_r^{(i)}$, velocity $\mathbf{u}_r^{(i)}$, and intensity $\mathbf{I}_r^{(i)}$).

2.3 Angle-dependent absorption coefficient

Based on the sound field separation defined in **Sec. 2.2**, the angle-dependent absorption coefficient can be determined according to [17]

$$\alpha(\theta) = \frac{P_{abs,\theta}}{P_{inc,\theta}} = 1 - \frac{\int_0^{2\pi}\left|\tilde{P}(\theta,\phi)\right|^2 d\phi}{\int_0^{2\pi}\left|\tilde{P}(\pi-\theta,\phi)\right|^2 d\phi}, \quad 0 \le \theta \le \frac{\pi}{2} \tag{5}$$

where $\left|\tilde{P}(\theta,\phi)\right|^2$ corresponds to the reflected power, and $\left|\tilde{P}(\pi-\theta,\phi)\right|^2$ to the incident power. As such, the estimation of absorption follows from the ratio of absorbed to incident power observed in the measurement aperture and does not assume any specific waveform incidence. The individual wavenumber spectra are integrated on the azimuth angle ϕ to prevent biases at angles with no incidence (a pure-tone sound field in a reverberation room is not diffuse, and not all frequencies contain energy in every direction [17]). This averaging procedure is not critical since, in the case of isotropic absorbers, the azimuth angle is of marginal significance [18].

3. EXPERIMENTAL RESULTS

This section describes measurements conducted in a large (215 m^3) reverberation room, using a programmable robotic arm to scan the sound field. Two damping conditions in the room were examined: the empty (undamped) room and the room with extra absorption (10.8 m^2 glass wool of thickness 100 mm and flow resistivity 12.9 kPa.s/m^2) on the floor. The room complies with the ISO 354 requirements, and is essentially box-shaped, although there are 85 built-in concrete boundary diffusers and 12 panel diffusers. A scanning robot UR5 (Universal Robot, Odense, Denmark) was programmed to move a free-field microphone (Brüel & Kjær, Nærum, Denmark) within a rectangular volume of dimension 0.6 x 0.8 x 0.25 m, creating a random array of 290 measurement positions in the vicinity of the absorbing sample (the closest microphone is located ~ 30 cm away from the absorber). The room was excited by a built-in loudspeaker driven with a logarithmic sine sweep ranging from 20 Hz to 20 kHz with a duration of 10 s. The frequency response was measured at the 290 positions with a spectral resolution of 0.1 Hz. The complex coefficient vector $\mathbf{x}$ corresponding to the wavenumber spectrum (i.e., the amplitudes of the waves) is estimated using Eq. (2). A plane-wave basis of 2000 plane waves of unknown amplitudes is considered, whose directions of propagation are distributed uniformly based on a Thomson problem. Tikhonov regularization (i.e., a l_2 least-squares solution) is used for the regularized inversion, along with the L-curve criterion as a parameter-choice method [21].

Figure 1 compares the magnitude of the wavenumber spectrum and corresponding spherical harmonic expansion at 1 kHz, measured in the undamped and damped rooms in the vicinity of the floor/absorber. In the undamped room, as seen in **Fig. 1(a)**, a few dominant directions are detected (i.e., a few waves carrying considerably more energy than others, seemingly corresponding to a few interfering modes and early reflections from the neighboring rigid floor), indicating that the field is not perfectly isotropic. In the damped room [added absorption, **Fig. 1(b)**], the wavenumber spectrum

is less omnidirectional, as there are no waves propagating in the positive z-direction (higher hemisphere in the wavenumber spectrum) because no sound is being reflected away from the absorber ($\alpha \approx 1$ at 1 kHz). Besides, the incident sound field (lower hemisphere) exhibits some dominant incident directions, indicating that the sound field incident onto the absorber is anisotropic. The results are supported by the corresponding spherical harmonics expansions: in the undamped case, the wavenumber spectrum is best described by the monopole moment of its spherical harmonic expansion although higher-order moments are required to explain the few dominant directions (the isotropy indicator in this case is $\iota = 0.43$, confirming that the sound field is not isotropic); in the damped case, the spherical harmonic expansion is no longer dominated by the monopole moment, resulting in a sound field that is less isotropic than in the undamped case ($\iota = 0.28$). It can be remarked that the isotropy indicator values are lower than in Ref. 15 for the same room/frequency, because the array is closer to the floor/absorber in this case. Another observation that can be drawn from these data is that there are clear differences between the two incident fields (with and without the sample - lower hemispheres in the wavenumber spectra), which demonstrates the effect of the absorber on the incident sound field.

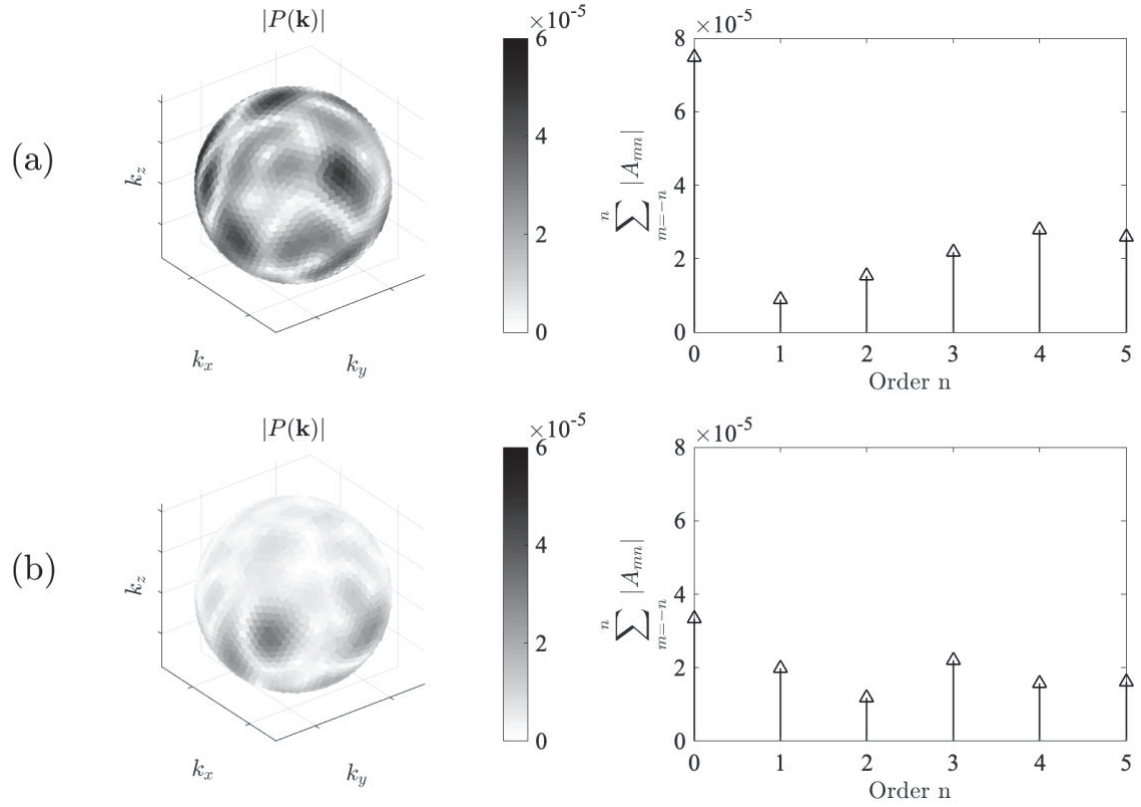

Figure 1 – Magnitude of the wavenumber spectrum and corresponding spherical harmonics expansion in (a) the undamped room; (b) the damped room. Frequency: 1 kHz. Truncation order: $N = 5$.

Figure 2 shows a volumetric reconstruction of the acoustic intensity *incident* onto the sample for selected third-octave bands (250 Hz, 500 Hz, 1 kHz, and 2 kHz).The incident active intensity vectors are computed over a parallelepiped lattice of 252 points in the vicinity of the absorbing plane (9 x 7 x 4 grid with lattice spacing of 10 cm). The length of the vectors is proportional to the intensity (in W/m^2) at the base of the cone, and the cones are color-coded to also show the magnitude of the intensity vectors. At all frequencies, the incident energy is not constant and uniform throughout space (in clear disagreement with theoretical predictions that follow from assuming at diffuse sound field). It should be remarked that the direction of incident energy flow is in general not in the direction of a single wave front, but rather results from the interaction of the many superposed waves; as such, it does not indicate the directional distribution of sound waves arriving onto a sample (contrarily to the wavenumber spectrum representation). Nevertheless, analysis of incident intensity can indicate the departure from the ideal state of diffusion.

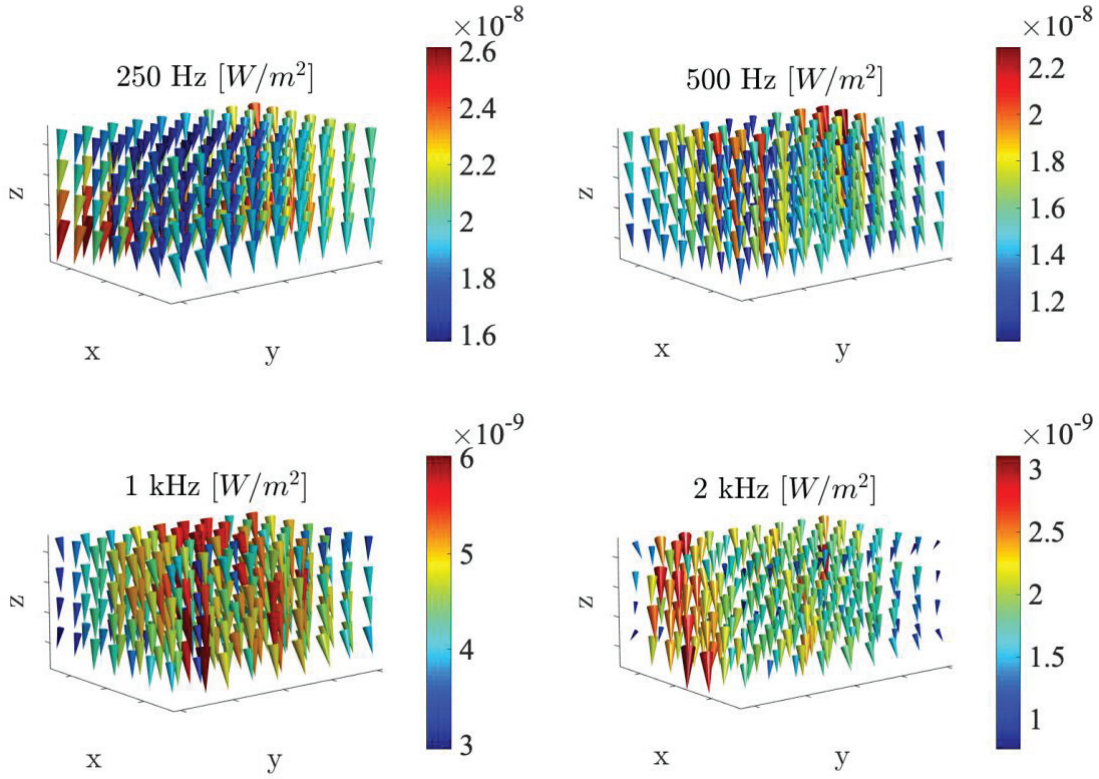

Figure 2 – Volumetric reconstruction of the active intensity *incident* onto the absorbing sample for selected third-octave bands. [Adapted from Ref. 17].

Figure 3 shows the angle-dependent absorption coefficient determined from the wavenumber spectrum measurement for the third-octave bands ranging from 200 Hz to 1 kHz. The absorption coefficient is averaged over the azimuth angle and calculated as mean values per third-octave bands. As mentioned in Sect. 2.3, the frequency averaging is performed on the wavenumber spectrum to avoid biased estimates. The asterisks * represent the experimental data estimated every 6° (π/30 rad). The solid line is calculated from a transfer matrix model in the case of a single layer of porous material with a rigid backing [22]. The characteristic impedance and the wavenumber for the material are obtained from Miki's empirical model [23]. The experimental values fit reasonably well with the prediction. The agreement is particularly good in the frequency range between 315 Hz and 1 kHz and for angles between 0 and 60° (π/3 rad). At lower frequencies, the incident energy is not uniformly distributed with angle, and the spatial resolution of the array is limited. At frequencies above 500 Hz, where the sample is highly absorptive, the absorption coefficient at grazing incidence is underestimated as a result of the limited wavenumber resolution of the measurement system: some of the incident energy on the absorber at grazing incidence (in the lower hemisphere of the wavenumber spectrum) leaks into the upper half of the wavenumber, which corresponds to directions of reflected components.

4. SUMMARY AND DISCUSSION

The directional properties of the reverberant sound field can be characterized by analyzing the wavenumber spectrum, which results from expanding the sound field into a plane-wave basis. Measurements in a standardized reverberation chamber show that the sound field is not isotropic (i.e., the wavenumber spectrum is not spherically/hemispherically symmetrical). The accuracy of the estimation depends on (i) the measurement system (the sampling of the pressure field should be sufficient to estimate the wavenumber spectrum correctly; yet, no specific array configuration is required); (ii) the choice of the regularization scheme. It can also be remarked that in a reverberation chambers with diffusing elements (such as panel or boundary diffusers), exponentially attenuated

waves (evanescent waves) will appear at the observation point, if the latter is located in close proximity of the diffusers. Besides, evanescent waves can be caused by diffraction evoked at the sample edges. This work is however concerned with analyzing the sound field away from any source and diffracting element (that is, evanescent waves are *not* present) [18].

The isotropy of a sound field can be characterized by expanding the wavenumber spectrum in the spherical harmonics domain, and the relative monopole strength determines the degree of isotropy. Yet, such quantitative indicator alone is of no help in interpreting the results. For example, it cannot distinguish between anisotropy due to low modal density and anisotropy caused by non-uniform placement of absorbing material. In this connection, the inspection of the wavenumber spectrum [e.g., **Fig. (1)**] is much more informative. The proposed measure may nevertheless be useful for comparative investigations in a given room (the influence of source position, diffusers placement, etc. can be examined). Note however that the metric is not a full measure of the degree of diffusion, since it disregards the correlation between waves incoming from different directions.

Measurement of the wavenumber spectrum makes it possible to reconstruct and characterize the incident energy flows over a three-dimensional domain. Measurement results confirm that the incident flow is not constant and uniform throughout space despite the presence of diffusing elements. This can be attributed to the coupling between the measuring sample and the sound field in its vicinity. The complex intensity vectors in a room can also be determined and visualized, which provides a valuable tool for understanding the relation between flows of net energy (active intensity) and oscillating energy (reactive intensity) in an empty reverberation chamber or with absorption on the floor.

Finally, the angle-dependent absorption coefficient (averaged over the azimuth angle) can be determined from measurement of the wavenumber spectrum in front of an absorbing plane. There is fair agreement with theoretical predictions.

It is anticipated that the experimental methods outlined in this paper may find application in measurements in ordinary rooms (especially in rooms with absorbent ceilings, e.g., classrooms, offices, etc.). The ability to characterize the spatial properties of the sound field in theses rooms may supplement reverberation time measurements in tasks related to room acoustical design.

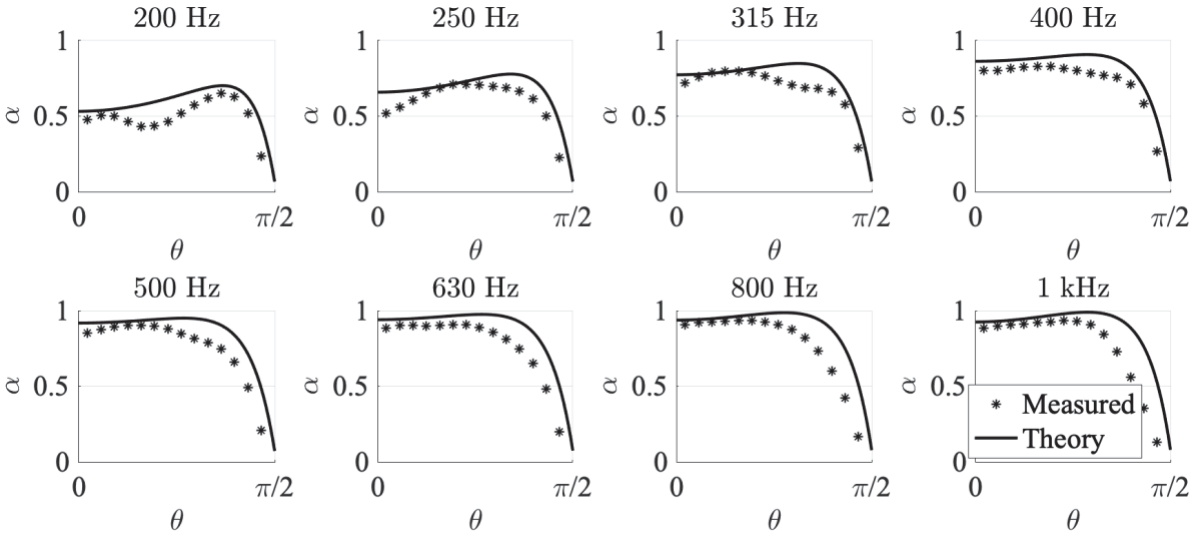

Figure 3 – Angle-dependent absorption coefficient determined from wavenumber spectrum measurements. The asterisks * represent experimental data; the solid line is obtained from a transfer matrix method along with Miki's model. [Adapted from Ref. 17].

ACKNOWLEDGEMENTS

This work was supported by the Oticon Foundation.

REFERENCES

1. ISO 354:2003: *Measurement of Sound Absorption in a Reverberation Room* (International

Organization for Standardization, Geneva, Switzerland, 2003).
2. W. C. Sabine, *Collected Papers on Acoustics* (Cambridge, Harvard University Press, 1922).
3. P. M. Morse and K. U. Ingard, *Theoretical Acoustics* (McGraw-Hill, New York, 1968), Sec. 9.5.
4. C. W. Kosten, "International comparison measurements in the reverberation room," Acustica **10**, 400-411 (1960).
5. Y. Makita, M. Koyasu, M. Nagatu, and S. Kimura, "Investigation into the precision of measurement of sound absorption coefficients in a reverberation room," J. Acoust. Soc. Jpn. **24**, 381-392 (1968).
6. R. E. Halliwell, "Inter-laboratory variability of sound absorption measurement," J. Acoust. Soc. Am. **73**(3), 880-886 (1983).
7. M. Nolan, M. Vercammen, C. -H. Jeong, and J. Brunskog, "The use of a reference absorber for absorption measurements in a reverberation chamber," in Proceedings of Forum Acusticum 2014, Krakow, Poland (2014).
8. T. J. Schultz, "Diffusion in reverberation rooms," J. Sound Vib. **16**, 17-28 (1971).
9. C. -H. Jeong, M. Nolan and J. Balint, "Difficulties in comparing diffuse sound field measures and data/code sharing for future collaboration," in Proceedings of Euronoise 2018, Heraklion, Crete (2018).
10. R. Thiele, "Richtungsverteilung und Zeitfolge der Schallrückwurfe in Räumen," Acustica **3**, 291-302 (1953).
11. E. Meyer and R. Thiele, "Raumakustische Untersuchungen in zahlreichen Konzertsälen und Rundfunkstudios unter Anwendung neuerer Messverfahren," Acustica, 6-425 (1956).
12. Y. Yamasaki and T. Itow, "Measurement of spatial information in sound fields by closely located four-point microphone method," J. Acoust. Soc. Jpn. (E) **10**, 101-110 (1989).
13. K. J. Ebeling, "Statistical properties of random wave fields," in *Physical Acoustics, Principles and Methods*, edited by W. P. Mason and R. N. Thurston (Academic, New York, 1984), Vol. XVII, Chap. 4, pp. 233-310.
14. B. N. Gover, J. Ryan, and M. Stinson, "Measurements of directional properties of reverberant sound fields in rooms using a spherical microphone array," J. Acoust. Soc. Am. **116**(4), 2138-2148 (2004).
15. M. Nolan, E. Fernandez-Grande, J. Brunskog, and C.-H. Jeong, "A wavenumber approach to quantifying the isotropy of the sound field in reverberant spaces," J. Acoust. Soc. Am. **143**(4), 2514-2526 (2018).
16. M. Berzborn and M. Vorländer, "Investigations on the directional energy decay curves in reverberation rooms," in Proceedings of Euronoise 2018, Heraklion, Crete (2018).
17. M. Nolan, S. A. Verburg, J. Brunskog, and E. Fernandez-Grande, "Experimental characterization of the sound field in a reverberation room," J. Acoust. Soc. Am. **145**(4), 2237-2246 (2019).
18. M. R. Schroeder, "Measurement of sound diffusion in reverberation chambers," J. Acoust. Soc. Am. **31**(11), 1407-1414 (1959).
19. E. G. Williams, *Fourier Acoustics: Sound Radiation and Near-Field Acoustical Holography* (Academic Press, New York, 1999).
20. E. Fernandez-Grande, "Sound field reconstruction using a spherical microphone array," J. Acoust. Soc. Am. **139**, 1168-1178 (2016).
21. P. C. Hansen, *Discrete Inverse Problems: Insight and Algorithms* (*Fundamental of Algorithms, Vol. 7*) (SIAM, Philadelphia, PA, 2010).
22. J. -F. Allard, *Propagation of Sound in Porous Media: Modelling Sound Absorbing Materials* (Elsevier Science Publishers, Amsterdam, the Netherlands, 1993), p. 38.
23. Y. Miki, "Acoustical properties of porous materials – Modifications of Delany-Bazley models," J. Acoust. Soc. Jpn. **11**, 19-24 (1990).